

## SEARCHING FOR PLANETS IN THE HYADES II: SOME IMPLICATIONS OF STELLAR MAGNETIC ACTIVITY <sup>1</sup>

DIANE B. PAULSON

Astronomy Department, University of Texas, Austin, TX 78712  
apodis@astro.as.utexas.edu

STEVEN H. SAAR

Center for Astrophysics, 60 Garden Street, Cambridge, MA 02138  
ssaar@cfa.harvard.edu

WILLIAM D. COCHRAN

McDonald Observatory, University of Texas, Austin, TX 78712  
wdc@astro.as.utexas.edu

AND

ARTIE P. HATZES

Thüringer Landessternwarte Tautenburg, D-07778 Tautenburg, Germany  
*To appear in the July 2002 issue of The Astronomical Journal*

### ABSTRACT

The Hyades constitute a homogeneous sample of stars ideal for investigating the dependence of planet formation on the mass of the central star. Due to their youth, Hyades members are much more chromospherically active than stars traditionally surveyed for planets using high precision radial velocity techniques. Therefore, we have conducted a detailed investigation of whether magnetic activity of our Hyades target stars will interfere with our ability to make precise radial velocity ( $v_{\text{rad}}$ ) searches for substellar companions. We measure chromospheric activity (which we take as a proxy for magnetic activity) by computing the equivalent of the  $R'_{\text{HK}}$  activity index (which is corrected for photospheric contributions), from the Ca II K line.  $\langle R'_{\text{HK}} \rangle$  is not constant in the Hyades: we confirm that it decreases with increasing temperature in the F stars, and also find it decreases for stars cooler than mid-K. We examine correlations between simultaneously measured  $R'_{\text{HK}}$  and radial velocities using both a classical statistical test and a Bayesian odds ratio test. We find that there is a significant correlation between  $R'_{\text{HK}}$  and the radial velocity in only 5 of the 82 stars in this sample. Thus, simple  $R'_{\text{HK}} - v_{\text{rad}}$  correlations will generally not be effective in correcting the measured  $v_{\text{rad}}$  values for the effects of magnetic activity in the Hyades. We argue that this implies *long timescale* activity variations (of order a few years; i.e., magnetic cycles or growth and decay of plage regions) will not significantly hinder our search for planets in the Hyades if the stars are closely monitored for chromospheric activity. The trends in the radial velocity scatter ( $\sigma'_v$ ) with  $\langle R'_{\text{HK}} \rangle$ ,  $v \sin i$ , and  $P_{\text{rot}}$  for our stars is generally consistent with those found in field stars in the Lick planet search data, with the notable exception of a shallower dependence of  $\sigma'_v$  on  $\langle R'_{\text{HK}} \rangle$  for F stars.

*Subject headings:* clusters: open (Hyades) — stars: planetary systems — techniques: radial velocities  
— stars: chromospheres — stars: activity

### 1. INTRODUCTION

The high-precision radial velocity ( $v_{\text{rad}}$ ) technique (e.g., Butler et al. (1996)) has been remarkably successful in discovering planetary-mass companions to nearby main-sequence stars. Studying these systems enables us to begin to place important new constraints on the planet formation process. So far, high precision radial velocity surveys have primarily targeted the brightest, and hence the nearest chromospherically inactive, slowly-rotating solar-type stars. Thus, while the targets cover a wide range of ages, compositions, and perhaps histories, they are dominated by old, higher mass stars.

A more complete understanding of the planet formation process hinges upon determining which stellar properties influence planetary system formation and dynamics. This can be accomplished with a well controlled and homoge-

neous sample of target stars. By varying only one stellar parameter at a time, we may begin to understand the properties and processes which govern planet formation.

We have been searching for planets in the Hyades cluster since 1996 (Cochran et al. (2001), hereafter Paper I). The Hyades cluster provides a uniform sample of stars in age and initial metallicity. Stellar mass is the main independent variable among the members. Thus, if planetary systems are found, we will easily be able to study the role stellar mass plays in the planet formation process.

In order to detect planetary systems, the  $v_{\text{rad}}$  signature must be unambiguous, and we must be certain it is due to an orbiting body and not intrinsic to the star. Several groups have explored the implications of intrinsic stellar properties, in particular stellar pulsations (Gray &

<sup>1</sup> Data presented herein were obtained at the W.M. Keck Observatory, which is operated as a scientific partnership among the California Institute of Technology, the University of California and the National Aeronautics and Space Administration. The Observatory was made possible by the generous financial support of the W.M. Keck Foundation.

Hatzes 1997), rotational velocity, and chromospheric activity (Saar & Donahue 1997; Saar et al. 1998; Santos et al. 2000a) on radial velocity measurements. Stellar non-radial (as well as radial) pulsation can easily give observable radial velocity variation, but may be distinguished from orbital motion by their resulting variations in stellar line bisectors (Gray & Hatzes 1997; Hatzes et al. 1997; Hatzes et al. 1998a,b; Brown et al. 1998b,a). The rotational modulation and evolution of velocity structures or non-uniform active regions can cause similar  $v_{\text{rad}}$  signatures to orbiting planets. Walker et al. (1992) showed that in the case of  $\gamma$  Cep, the  $v_{\text{rad}}$  measurements suggestive of a planet were instead likely due to rotation of active regions seen in equivalent widths of the Ca II 8662 Å line. Walker et al. (1995) detected a correlation between  $v_{\text{rad}}$  and long-term Ca II emission variations in  $\kappa^1$  Ceti probably due to its magnetic cycle. Queloz et al. (2001) showed that the apparent radial velocity signal in HD 166435, which was originally interpreted as due to a planetary companion is actually correlated with photospheric line profile variations and is best explained by the presence of dark photospheric spots. Dravins & Nordlund (1990) discussed the possibility of apparent false Doppler shifts over the course of a stellar activity cycle, though, McMillan et al. (1993) has shown that solar cycle magnetic variations are undetectable in disk integrated spectra of the sun. Saar and collaborators (Saar et al. 2002; Pearson et al. 2000; Saar & Fischer 2000; Saar & Snyder 1999) are working on methods for correcting stellar radial velocities to compensate for the stellar activity, but these techniques are still under development. Because of worries about such activity-related  $v_{\text{rad}}$  noise, past planet surveys have been biased against young, active stars (Vogt et al. 2002; Henry et al. 1997; Saar & Donahue 1997). Consequently, out of 76 planets discovered as of December 2001, only four have been found around young, active stars:  $\epsilon$  Eridani (Hatzes et al. 2000),  $\iota$  Horologii (Kürster et al. 2000), HD 192263 (Santos et al. 2000a), and GJ 3021 (Naef et al. 2001).

Because the Hyades cluster is so young ( $625 \pm 50$  Myr; Perryman et al. (1998)), the stars can be quite active. Thus, we must determine if this activity is a major contributor to the observed  $v_{\text{rad}}$  variances. In this paper, we explore the connection between activity variations and radial velocity measurements in Hyades stars by looking for correlations between the Ca II K emission and the  $v_{\text{rad}}$  (measured in the same spectra). This will help us understand to what degree this phenomenon masks or complicates detection of the low velocity signal induced by planetary mass companions.

## 2. OBSERVATIONS AND ANALYSIS

We are conducting a radial velocity survey of Hyades dwarfs using the Keck HIRES spectrograph to search for Jupiter and Saturn-mass companions (see Paper I). By using a 10m class telescope, we are able to study even low mass Hyads (down to  $M \approx 0.4M_{\odot}$ ). So far, this survey has produced a number of stars showing rms velocity variation significantly larger than the internal velocity uncertainty ( $\sigma_i$ , which includes instrumental noise, photon noise, and increased noise due to observational effects such as reduced line density and depth in F stars and increased line width in stars with higher  $v \sin i$ ). Unfortunately, the scheduling

of our observing time on Keck has made it impossible to sample short periods without significant aliasing. We began observations of short period candidates with the High Resolution Spectrograph on the Hobby-Eberly Telescope in the fall of 2001.

### 2.1. Sample

Our total sample consists of 98 Hyades dwarfs ranging from F5 to M2. All of the targets are confirmed members according to Perryman et al. (1998), and all known spectroscopic binaries have been removed. We imposed a stellar rotational velocity limit of  $v \sin i \leq 15 \text{ km s}^{-1}$ . For the chromospheric activity study presented here, we neglect all stars with fewer than six observations, reducing the sample to 82 stars.

### 2.2. $v_{\text{rad}}$ measurements

The observations at Keck I make use of the HIRES (Vogt et al. 1994) with I<sub>2</sub> gas absorption cell as a standard velocity reference (Valenti et al. 1995) as detailed in Paper I. S/N $\sim$ 300 is required in this configuration (at resolution  $R \simeq 60,000$ ) to obtain  $v_{\text{rad}}$  precision (in the best cases) of  $\sim 3 \text{ m s}^{-1}$  (see Paper I); S/N $\sim$ 100 yields precision of  $\sim 5\text{-}6 \text{ m s}^{-1}$ . In addition, the exposure times must be kept to  $\leq 15$  minutes. We use standard IRAF packages to reduce the CCD images and extract the observed spectra.

It is useful to explore how the rotational broadening in the spectra affects the internal  $v_{\text{rad}}$  errors ( $\sigma_i$ ). Since we have preselected stars with  $v \sin i \leq 15 \text{ km s}^{-1}$ , we only have a small range of  $v \sin i$  to study. In Figure 1, we show the relationship between  $v \sin i$  (taken from the literature as referenced in Table 1) and the mean internal errors ( $\langle \sigma_i \rangle$ ) we achieve. Stars with only  $v \sin i$  upper limits have not been included in the analysis. Error bars on  $\langle \sigma_i \rangle$  indicate the rms about the mean. We note that even with this limited set of data, we see the trend that one would expect; that increasing  $v \sin i$  degrades our velocity precision, due to the lowered precision in determining the center of broader lines. In order to estimate how large our errors are at  $v \sin i = 15 \text{ km s}^{-1}$ , we fit a linear relation to the data. We find

$$\langle \sigma_i \rangle = 1.050 + 0.555 * v \sin i \text{ m s}^{-1}. \quad (1)$$

Therefore, at the cutoff of  $15 \text{ km s}^{-1}$ , we can still achieve  $v_{\text{rad}}$  precision of  $\sim 10 \text{ m s}^{-1}$ . We would like to point out that these are our *mean* internal errors of all of our spectra of a given star. If instead we had chosen the highest S/N spectrum, we would have derived  $\sigma_i = 6.5 \text{ m s}^{-1}$  at  $v \sin i = 15 \text{ km s}^{-1}$ . For  $v \sin i \lesssim 3 \text{ km s}^{-1}$ , other sources of line broadening become important (e.g., macroturbulence), and  $\langle \sigma_i \rangle$  is no longer dominated by  $v \sin i$ .

### 2.3. Calibration of Chromospheric Activity

Most stellar chromospheric activity is attributed to the interaction of magnetic fields with convection (Middelkoop & Zwaan 1981; Tinbergen & Zwaan 1981; Middelkoop 1982). However, the effect of magnetic processes on the integrated radial velocity of a star at the few  $\text{m s}^{-1}$  level is only beginning to be explored. To date, stars which are chromospherically active and show no obvious trend in the velocity signal over a given timescale are either observed less frequently or removed from planet surveys (Vogt et al.

2002; Cumming et al. 1999; Saar & Donahue 1997). This is because these stars tend to show somewhat higher levels of radial velocity scatter, attributed to the magnetic activity, and this will possibly inhibit detection of low-amplitude velocity signals.

The question arises as to whether stellar activity in Hyades stars induce significant periodic centroid shifts in photospheric absorption lines, and thus  $v_{\text{rad}}$  signals which could be confused for perturbations made by planetary companions. The members of the Hyades cluster are chromospherically active, and quite young. Because activity might be a significant source of radial velocity variation (Saar & Donahue 1997; Saar et al. 1998; Saar & Fischer 2000), we include the Ca II H & K lines in the spectral region of each exposure for velocity measurement with the Keck HIRES. We have monitored the chromospheric activity of our target stars, acquiring Ca II K emission core flux measurements simultaneously with each velocity measurement.

To measure stellar chromospheric activity, the Mt. Wilson  $S$  index is adopted. This index is defined (e.g. Baliunas et al. (1995)) as a quantity proportional to the sum of the flux in  $1\text{\AA}$  FWHM triangular bandpasses centered on the Ca II H and K lines divided by the sum of the flux in  $20\text{\AA}$  bandpasses in the continuum at  $3901\text{\AA}$  and  $4001\text{\AA}$  (Soderblom et al. 1991; Baliunas et al. 1995).

At Keck 1, we set HIRES so that the Ca II H and K lines are contained within the spectra for all stars observed. The four quantities to be measured (the two calcium line core fluxes plus the two continuum bandpass fluxes) are spread across three echelle spectral orders which overlap by a few  $\text{\AA}$ . As a result of flat fielding uncertainties in the most blueward order, we do not use measurements in this order, i.e. of the blue ( $3901\text{\AA}$ ) continuum. In addition, we do not measure the Ca II H line (at  $3968.47\text{\AA}$ ) because for some stars, the wings of strong Balmer H $\epsilon$  features (at  $3970.07\text{\AA}$ ) lay within the measured bandpass. This would affect measurement of the Ca II H line flux as the absorption can be strong enough so as to artificially decrease the Ca II H flux, and strong H $\epsilon$  emission (seen in a few of the M dwarfs) will artificially increase the measured Ca II H line flux. Therefore, we have defined an index  $S_{\text{Keck}}$  which is the ratio of the flux in a  $1\text{\AA}$  triangular bandpass centered on the Ca II K line to the flux in a  $20\text{\AA}$  bandpass centered on the redward continuum at  $4001\text{\AA}$ . Figure 2 shows the numerical filter we used in measuring the Ca II K flux. Several of our Hyades program stars have previously been measured as part of the Mt. Wilson program (Duncan et al. 1984). In Figure 3, we show the relationship between our  $S_{\text{Keck}}$  and  $S_{\text{Duncan}}$  (the published mean  $S$  data for stars measured by Duncan et al. (1984) including error bars which characterize the rms of the measured  $S$  index over the course of observations (including variability)). We find the linear relation

$$S_{\text{Duncan}} = -0.027(\pm 0.046) + 0.991(\pm 0.120)S_{\text{Keck}} \quad (2)$$

Both the slope and the intercept of the formal fit are within  $1\sigma$  of  $S_{\text{Keck}} = S_{\text{Duncan}}$ . We are thus able to transform our data into a standard Mt. Wilson  $S$  index scale using Equation 2. We call our transformed values  $S_{\text{MW}}$ .

In addition, we further transform our chromospheric  $S$  index to  $R'_{\text{HK}} = F'_{\text{HK}}/F_{\text{bol}}$ , where  $F'_{\text{HK}}$  is the Ca II HK surface flux, corrected for flux contributions from the pho-

tosphere, and  $F_{\text{bol}}$  is the bolometric flux (Noyes et al. 1984; Middelkoop 1982). Thus,  $R'_{\text{HK}}$  is the normalized, purely chromospheric component of the HK flux and is also useful as a means to compare stars of different spectral types. To convert from  $S_{\text{MW}}$  to  $R'_{\text{HK}}$ , we used the method outlined in Noyes et al. (1984), with  $B - V$  color index of each star obtained from Allende Prieto & Lambert (1999), and no reddening corrections were used.

### 3. RESULTS

#### 3.1. Chromospheric activity

Figure 4 shows the variation of  $\langle R'_{\text{HK}} \rangle$  with  $B - V$  for our sample of Hyades dwarfs. This demonstrates that activity as measured by  $\langle R'_{\text{HK}} \rangle$  is *not* constant with  $B - V$  in Hyades stars:  $\langle R'_{\text{HK}} \rangle$  values decrease from a plateau with  $\langle \log R'_{\text{HK}} \rangle \approx -4.42$  for  $B - V < 0.7$  and for  $B - V > 1.1$ . Noyes et al. (1984) notes that the values of  $R'_{\text{HK}}$  for  $B - V > 1.0$  may be uncertain by as much as 20%. However, the downward trend of  $B - V$  below 0.7 has not yet been addressed to our knowledge. A few outliers with  $B - V < 0.7$  (see Fig. 4) were determined not to be Hyades members by D. Latham (private communication) based on too large Hipparcos distances, photometry below main sequence and velocities which disagree with members, in contrast to Perryman et al. (1998) who found these same stars to be members. The decline for  $B - V < 0.7$  confirms the trend observed by Duncan et al. (1984) and Soderblom (1985) and seen in the data collected by Rutten (1987). HK data for the younger Pleiades cluster (age  $\sim 0.1$  Gyr) shows more scatter (Rutten 1987), but a similar, though weaker, decline for  $B - V < 0.7$ . This suggests that the decline in activity for  $B - V < 0.7$  is real (as opposed to a problem in  $R'_{\text{HK}}(B - V)$  calibration); a color-dependent calibration error should not evolve significantly between the ages of the Pleiades and Hyades. Thus, although we must be cautious about stars with  $B - V > 1.0$ , we confirm that at fixed age, there is a broad maximum in chromospheric emission for  $0.7 \leq B - V \leq 1.0$  ( $\approx G5$  to  $K3$ ), with decreases for both hotter and (tentatively) for cooler stars.

#### 3.2. Intrinsic $v_{\text{rad}}$ Jitter

##### 3.2.1. Comparison of Observed $v_{\text{rad}}$ Jitter with Empirical Relations

Saar et al. (1998) (hereafter SBM) used the observed radial velocity dispersion ( $\sigma_v$ ) in the Lick planet search data to compute the  $v_{\text{rad}}$  dispersion above the internal errors,  $\sigma'_v = (\sigma_v^2 - \sigma_i^2)^{0.5}$ . They then searched for correlations between  $\sigma'_v$  and  $\langle R'_{\text{HK}} \rangle$ , rotational period ( $P_{\text{rot}}$ ), and projected rotational velocity ( $v \sin i$ ). They also developed a simple model based on rotating/evolving starspots and plage to predict  $\sigma'_v$ . The Hyades dwarfs studied here are significantly more active on average than those stars studied in SBM, making it useful to investigate whether Hyad  $\sigma'_v$  behave similarly. We calculated  $\sigma'_v$  in the same manner as SBM, removing internal noise from each measurement. Due to the selection of stars with  $v \sin i \leq 15$   $\text{km s}^{-1}$  (Paper I), we have also selected for stars with low radial velocity jitter as shown in the model developed in SBM. We have also ignored stars with very large ( $\gg 100$   $\text{m s}^{-1}$ ) systematic velocity trends. F stars in our sample (ignoring one outlier) have  $\sigma'_v$  ranging from  $\sim 8$  to  $38$   $\text{m s}^{-1}$ .

$s^{-1}$  with an average value of  $\langle\sigma'_v\rangle = 14.8 \pm 8.4 \text{ m s}^{-1}$ , G stars range from  $\sim 5$  to  $40 \text{ m s}^{-1}$  ( $\langle\sigma'_v\rangle = 18.9 \pm 9.0 \text{ m s}^{-1}$ ), K stars (ignoring one outlier) range from  $\sim 3$  to  $45 \text{ m s}^{-1}$  ( $\langle\sigma'_v\rangle = 14.2 \pm 13.6 \text{ m s}^{-1}$ ), and M stars from  $\sim 4$  to  $20 \text{ m s}^{-1}$  ( $\langle\sigma'_v\rangle = 12.7 \pm 7.6 \text{ m s}^{-1}$ ).

A comparison of the observed  $\sigma'_v$  and the values predicted by empirical relationships found in the Lick  $v_{\text{rad}}$  database ( $\sigma'_v(\text{pred})$ ; see SBM) are shown in Fig. 5 (first three panels) and summarized in Table 2. For the rotation-related quantities,  $P_{\text{rot}}$  and  $v \sin i$ , agreement is generally quite good, with the scatter  $\sigma$  about the line  $\sigma'_v = \sigma'_v(\text{pred})$  at or below the values found for the empirical SBM fits. (We have considered only stars with measured  $P_{\text{rot}}$ .) Stars with only upper limits to  $v \sin i$  are also all in agreement with predictions.

Only relatively few Hyades stars have measurements of  $P_{\text{rot}}$  and  $v \sin i$  needed to compare  $\sigma'_v$  with the predictions of  $\sigma'_v(\text{pred})$  based on these parameters using the SBM results. With  $\langle R'_{\text{HK}} \rangle$  though, all the Hyades sample can be used except M stars (which were not studied in SBM). If  $\sigma'_v(\text{pred})$  is predicted using  $R'_{\text{HK}}$  and the combined Lick G and K star sample, the scatter  $\sigma_{rms}$  of Hyades G and K stars'  $\sigma'_v$  about this  $\sigma'_v(\text{pred}) (R'_{\text{HK}}(\text{G+K}))$  is slightly higher than for the Lick stars. This is true even if one Hyades outlier (a K star) is removed ( $\sigma_{rms}(\text{Hyades}) = 0.28$  dex compared with  $\sigma_{rms}(\text{Lick}) = 0.25$ ). To explore this result further, we compared  $\sigma'_v$  for the Hyad G and K stars separately with  $\sigma'_v(\text{pred}) (R'_{\text{HK}}(\text{G+K}))$ , and also with  $\sigma'_v(\text{pred})$  based on separate empirical fits to the Lick G and K stars (not published in SBM). These tests indicate that  $\sigma_{rms}(\text{Hyades})$  is smaller than  $\sigma_{rms}(\text{Lick})$  for the G stars ( $\approx 0.22$  dex), whether  $\sigma'_v$  is compared to  $\sigma'_v(\text{pred}) (R'_{\text{HK}}(\text{G+K}))$  or  $\sigma'_v(\text{pred}) (R'_{\text{HK}}(\text{G}))$ . The scatter is notably worse for K stars, though improved somewhat with the separate K star empirical fit:  $\sigma_{rms} \approx 0.32$  dex using  $\sigma'_v(\text{pred}) (R'_{\text{HK}}(\text{G+K}))$ ,  $\sigma_{rms} \approx 0.28$  dex using  $\sigma'_v(\text{pred}) (R'_{\text{HK}}(\text{K}))$ , with one outlier removed in each case. Thus, since F, G, and K stars are best fit when treated separately, the Hyades  $\sigma'_v$  data suggest a systematic spectral type dependence in the relationship between  $\sigma'_v$  and  $R'_{\text{HK}}$ .

The Hyades F stars (excluding one outlier) show a systematic trend relative to the  $\sigma'_v = \sigma'_v(\text{pred})$  line which suggests the empirical relation ( $\sigma'_v(\text{F}) \propto \langle R'_{\text{HK}} \rangle^{1.7}$ ; SBM) may be too steep. Indeed, the scatter is lower and the trend largely removed if the relations for G or G+K stars are used instead ( $\sigma_{rms} = 0.21$  dex or  $0.28$  dex, respectively, compared with  $\sigma_{rms} = 0.38$  dex using the F star fit). The  $v \sin i \leq 15 \text{ km s}^{-1}$  limit of our sample, though, may be a factor; while this limit has little effect on G and K Hyades stars, it definitely excludes some high  $v \sin i$  (and hence high  $R'_{\text{HK}}$ ) F stars. The Lick analysis was performed without any  $v \sin i$  restrictions, and includes two F stars with  $v \sin i \geq 15 \text{ km s}^{-1}$ . Restrictions on  $v \sin i$  will tend to limit  $\sigma'_v$  for a fixed  $R'_{\text{HK}}$ , since the higher  $v \sin i$  is an important component for enhanced  $v_{\text{rad}}$  noise (Saar & Donahue 1997).

The two ‘‘outlier’’ stars noted above (one F and one K type) show  $\sigma'_v$  values significantly enhanced (by  $>$

$2\sigma_{rms}(\text{Lick})$ ) over that predicted by  $\sigma'_v(\text{pred}) (R'_{\text{HK}})$ . Hence, these stars have large additional  $v_{\text{rad}}$  variations not associated with activity, and are particularly good candidates for further and more frequent observations in search of low mass companions.

### 3.2.2. Comparison of Observed $v_{\text{rad}}$ Jitter with a Simple Model

We have also compared Hyades  $\sigma'_v$  values with the combined spot/plage  $\sigma'_v$  model outlined in SBM. This model combines the rotating spot model from Saar & Donahue (1997) with a (very) simple plage model which assumes that convective velocity changes due to plage magnetic fields are  $\propto v_{\text{mac}}$ , the macroturbulent velocity. The full model is given by

$$\sigma'_v(\text{mod}) \approx \sqrt{[4.6 f_S^{0.9} (v \sin i) \cos(\theta)]^2 + [\alpha A(f_P) (v_{\text{mac}} + v \sin i)]^2} [\text{ms}^{-1}]. \quad (3)$$

Here,  $f_S$  is the *differential* spot filling factor (the portion of the total spot filling factor responsible for photometric variations). Also,  $\langle \theta \rangle$  is the mean spot latitude,  $\alpha$  is an adjustable constant, and  $A(f_P)$  is a function of the plage filling factor  $f_P$ , given by  $A(f_P) = 0.25 \sin(\pi \sqrt{f_P})$  (the scaling factor was not explicitly given in SBM; it scales the maximum of  $A(f_P) = f_P$ ). Following SBM, we take  $f_P = 0.08 (\tau_c / P_{\text{rot}})^{1.8} < 0.65$  (Saar (1996); where  $\tau_c$  is the convective turnover time from (Noyes et al. 1984)),  $\langle \theta \rangle = 45^\circ$ ,  $\alpha \approx 9$ , and estimate  $v_{\text{mac}}$  from relations for active stars in Saar & Osten (1997).

Unfortunately, only five stars had the required data ( $v \sin i$ ,  $P_{\text{rot}}$ , and photometry sufficient to estimate  $f_S$ ) to make a complete model estimate of  $\sigma'_v$ . If we assume  $f_S \approx 0$  for F stars (Hyades F stars show little photometric variability – Radick et al. (1998)) used them as constant check stars), and estimate their  $P_{\text{rot}}$  from  $R'_{\text{HK}}$  (vis. Noyes et al. (1984)) we gain two more stars. Several more have upper limits to  $v \sin i$ . As shown in Figure 5 (lower right) and Table 2, the agreement between  $\sigma'_v$  and  $\sigma'_v(\text{mod})$  for the (few!) stars we can model adequately is quite good:  $\sigma_{rms}$  is  $\approx 6$  to  $7 \text{ m s}^{-1}$  or  $\approx 0.13$  dex (comparable to SBM). All cases where only upper limits on  $\sigma'_v(\text{mod})$  are possible (due to  $v \sin i$  upper limits) are in agreement as well.

### 3.3. $R'_{\text{HK}}$ vs. $v_{\text{rad}}$

We have calculated the linear correlation coefficient ( $r$ ) in the standard way (Bevington & Robinson 1992) to search for any statistical correlations between the chromospheric activity and the radial velocity for each star. The values of  $r$  (which range from -1 to 1) calculated are shown in column 6 of Table 3. We then use this quantity to test statistically (both in a frequentist and a Bayesian manner) whether any linear correlations exist between the  $v_{\text{rad}}$  and  $R'_{\text{HK}}$ .

We first follow the frequentist approach given in Bevington & Robinson (1992) to determine a probability that the  $v_{\text{rad}}$  and  $R'_{\text{HK}}$  are correlated. The correlation coefficient is used to find a probability  $P_c$  that the data come from an uncorrelated parent population ( $P_c=1$  indicates that the data are completely uncorrelated, while  $P_c=0$  indicates be a completely correlated data set). The results from this test are in column 8 of Table 3. In using this method, we find several stars with high probabilities that the data come from a correlated parent sample. However, this method introduces a bias, since  $P_c$  is calculated by

only considering  $r$  relative to an uncorrelated parent sample. What is perhaps a better test is to compare the data to both correlated and uncorrelated parent samples. This way, we can test both hypotheses and make a better determination of possible correlation in the parent sample. To do this, we use a Bayesian approach.

Our Bayesian analysis uses an odds ratio ( $K$ ) defined by Jeffreys (1961). This incorporates prior knowledge of a probability distribution of  $r$  of the parent sample. Here, we choose a prior distribution to be constant and centered on (0,0). We calculate a ratio of the probability that  $v_{\text{rad}}$  and  $R'_{\text{HK}}$  are uncorrelated versus the probability that they are correlated (i.e.,  $K \ll 1$  indicates a strong correlation,  $K \gg 1$  the lack of one). For example, for  $K = 2$ , there are 2:1 odds that the sample is uncorrelated (i.e., a 67% chance that the sample is uncorrelated). Column 9 of Table 3 gives the odds ratios. However, Schmitt (1969) notes that the strength of correlations worked out in this manner is somewhat overestimated: correlation probabilities  $< 75\%$  are highly suspicious. In contrast to the frequentist correlation analysis, with the Bayesian techniques, we show that 15 stars have greater than 50% chance of being correlated. Of these, 5 show a strong chance of correlation-greater than 70%. Due to the small number of observations, Bayesian statistics will yield more reliable results, so these values are the ones the authors favor. Of the remaining stars, 40 show slight non-correlation between  $v_{\text{rad}}$  and  $R'_{\text{HK}}$  and 11 show slight correlation. So, the overwhelming majority of stars are slightly to strongly uncorrelated. Figures 6 and 7 show examples of stars with uncorrelated and correlated trends, respectively, from the previous analysis.

#### 4. DISCUSSION

Our fundamental result is that very few Hyads (5 of 82) show significant correlations between simultaneous  $v_{\text{rad}}$  and  $R'_{\text{HK}}$  measurements. It is therefore important to review how stellar activity can alter observed radial velocities, and what our result then implies for planet detection in the Hyades. In the Sun, Ca II emission primarily reflects the surface coverage of plage and active network, since it is relatively weak over sunspots themselves (e.g. Linsky & Avrett (1970) and references therein), and spot area is typically small relative to plage area. Thus,  $v_{\text{rad}}$  fluctuations due to spots (e.g., Saar & Donahue (1997)) will not have corresponding  $\Delta R'_{\text{HK}}$ , and so spots should not be a significant contributor to  $v_{\text{rad}} - R'_{\text{HK}}$  correlations. Plage/network can generate  $v_{\text{rad}}$  fluctuations in two main ways. First, plage is slightly brighter in the continuum (by a few %) than the quiet Sun. Assuming this is also true for stars, rotation of inhomogeneous patches of plage will cause traveling enhancements at the local intensity-weighted rotational velocity, which will translate into apparent  $v_{\text{rad}}$  changes on  $P_{\text{rot}}$  timescales. This effect is completely analogous to the one caused by spots. Since the brightness enhancement of plage is tiny compared with the  $\sim 90\%$  light deficit (in  $V$ ) due to sunspots, though, the brightness effect of plage on  $v_{\text{rad}}$  should be small, even considering the typically larger plage area.

To explore the effects on  $v_{\text{rad}}$ -activity correlations, consider that an identical plage, observed at two rotation angles  $\pm\phi$  (measured from disk center), will exhibit identical activity enhancements (i.e.,  $\Delta R'_{\text{HK}}(\phi) = \Delta R'_{\text{HK}}(-\phi)$ ),

but will show perturbations to  $v_{\text{rad}}$  due to brightness of opposite sign:  $\Delta v_{\text{rad}}(\phi) = -\Delta v_{\text{rad}}(-\phi) = \alpha v_{\text{rot}}(\phi)$  (where  $\alpha$  is some function of the plage brightness enhancement). Thus, a given plage will show a scatter of  $\Delta v_{\text{rad}}$  due to its brightness as it rotates across the disk. When averaged over enough observations, intensity changes due to activity (spots or plage) have no net  $v_{\text{rad}}$  effect, since the perturbations  $\propto \pm v_{\text{rot}}(\phi)$  will average to zero over the many observed  $\phi$ . Changing the mean level of activity will change the average magnitude of the effect and its rms, but once again, for sufficient  $\phi$  coverage the net  $\Delta v_{\text{rad}} = 0$ .

In addition to its brightness perturbation, plage also induces changes in the local velocity field, suppressing convective velocities in strong magnetic fields. The altered velocity field induces changes in the line shape (Livingston 1982) and leads to an overall convective blueshift in the Sun (Cavallini et al. 1985). Furthermore, these changes will vary from line to line based on their strength and excitation, just as line bisectors do (e.g., Asplund et al. (2000)). Thus, in the case of plage the  $v_{\text{rad}}$  perturbation may be written  $\Delta v_{\text{rad}}(\phi) = v_{\text{blue}}(\phi) + v_{\text{shape}}(\phi)$ , where  $v_{\text{blue}}(\phi)$  is the overall convective shift of the line core, and  $v_{\text{shape}}(\phi)$  is the apparent  $v_{\text{rad}}$  change due to the altered line profile shape. The latter arises because most methods measure the  $v_{\text{rad}}$  of individual exposures by comparison to a single high S/N “template” spectrum (either an average spectrum or a single deep exposure). Fluctuations in line shape relative to this “template” will inevitably lead to an apparent shift in the line centroid, and hence  $v_{\text{rad}}$ . In contrast with brightness perturbations, the time average of  $v_{\text{blue}}(\phi) + v_{\text{shape}}(\phi)$  will in general be non-zero, since both, due to their intimate connection with convection are (unlike  $v_{\text{rot}}$ ) symmetric about  $\phi = 0$  in the time-averaged sense. Clearly, *strong correlations between  $v_{\text{rad}}$  and  $R'_{\text{HK}}$  will result primarily from these long timescale changes in average plage area* (see also Saar & Fischer (2000)). The present results say little about short term (timescales  $\lesssim P_{\text{rot}}$ ) changes in  $v_{\text{rad}}$ , or about the effects of starspots.

The lack of many significant  $v_{\text{rad}} - R'_{\text{HK}}$  correlations in the Hyades thus implies that *longterm* changes in plage activity have little effect on  $v_{\text{rad}}$  for our stars. This is not an entirely surprising result. If we look at active stars in Balinas et al. (1995), relatively few show clear cycles in Ca II (see also Saar (2002)). Without a systematic long-term activity variation, active stars are less likely to show strong  $v_{\text{rad}} - R'_{\text{HK}}$  correlations. Typically, short term (rotational) jitter in  $v_{\text{rad}}$ , and perhaps flares in activity, are expected to dominate active stars without strong cycles, swamping potential  $v_{\text{rad}} - R'_{\text{HK}}$  correlations with rapid fluctuations in one or both variables. Thus, the method suggested by Saar & Fischer (2000) for correcting  $v_{\text{rad}}$  timeseries for some of the jitter induced by activity will not be effective for most Hyads. Other methods, based for example on variable line bisector changes (Saar et al. 2001; Saar et al. 2002; Queloz et al. 2001) may be useful in diagnosing (and possibly correcting) for short term  $v_{\text{rad}}$  jitter from spots and plages.

Clearly, the changing  $\langle R'_{\text{HK}} \rangle$  with  $B - V$  implies that the inverse Rossby number  $Ro^{-1} = \tau_C / P_{\text{rot}}$  (at least as defined by Noyes et al. (1984)) is not constant with mass at fixed age. This confirms and extends (to  $B - V > 1.0$ ) the

similar conclusion of Soderblom (1985). Consistent with this, the age calibration of Donahue, Dobson & Baliunas (1997), which estimates age  $t$  as a function of  $\langle R'_{\text{HK}} \rangle$  alone, predicts  $\langle \log t[\text{yr}] \rangle = 8.89 \pm 0.27$  (in agreement with Peryman et al. (1998)) but overestimates  $t$  for  $B - V < 0.60$  and  $B - V > 1.30$ . The physical implications of a mass dependent  $\langle R'_{\text{HK}} \rangle$  in the Hyades are less clear. Apparently, either generation of magnetic flux, or the physics of chromospheric heating, or both, vary with mass at fixed age. There is some independent evidence for both of these ideas. Saar (2001) finds a monotonic relation between magnetic flux and  $Ro^{-1}$ , which implies mass dependent magnetic flux in the Hyades, given that  $Ro^{-1}$  is not constant. Supporting the concept of mass-dependent changes in heating, several researchers (e.g., Rutten et al. (1989)) have noted that in comparison to hotter stars, M dwarfs show Balmer emission dominating over HK emission, and chromospheric emission in general reduced relative to coronal emission.

Taken as a whole, the  $\sigma'_v$  values for the Hyades are in reasonably good agreement with empirical results and models

in SBM. The main exceptions are that the Hyades data suggest a more continuous change in the dependence of the  $\sigma'_v - \langle R'_{\text{HK}} \rangle$  relationship on spectral type (e.g., G and K stars are better considered separately). Also, the SBM fit for F stars,  $\sigma'_v \propto \langle R'_{\text{HK}} \rangle^{1.7}$  may be too steep, as also suggested by Santos et al. (2000b). The difference may however be the result of the limitation of  $v \sin i \leq 15 \text{ m s}^{-1}$  in the present sample. Further analysis of the Lick and Hyades data, with and without  $v \sin i$  limits, is needed to resolve this issue.

We wish to thank Debra Fischer for many useful suggestions. We would also like to thank Chris Sneden and Bill Jefferys for several useful discussions on the topics of this paper. In addition, we are grateful to David Latham and Robert Stefanik for their assistance in identifying binary stars and Hyades non-members from our sample. DBP and WDC are supported by NASA grants NAG5-4384 and NAG5-9227 and NSF grant AST-9808980. SHS is supported by NASA grant NAG5-10630.

#### REFERENCES

- Allende Prieto, C. & Lambert, D. L. 1999, *A&A*, 352, 555  
 Asplund, M., Nordlund, A., Trampedach, R., Allende-Prieto, C., & Stein, R. 2000 *A&A*, 359, 729  
 Baliunas, S. L., Donahue, R. A., Soon, W. H., Horne, J. H., Frazer, J., Woodard-Eklund, L., Bradford, M., Rao, L. M., Wilson, O. C., Zhang, Q., Bennett, W., Briggs, J., Carroll, S. M., Duncan, D. K., Figueroa, D., Lanning, H. H., Misch, T., Mueller, J., Noyes, R. W., Poppe, D., Porter, A. C., Robinson, C. R., Russell, J., Shelton, J. C., Soyumer, T., Vaughan, A. H., & Whitney, J. H. 1995, *ApJ*, 438, 269  
 Bevington, P. R. & Robinson, D. K. 1992, *Data Reduction and Error Analysis for the Physical Sciences* (New York: McGraw-Hill)  
 Brown, T. M., Kotak, R., Horner, S. D., Kennelly, E. J., Korzennik, S., Nisenson, P., & Noyes, R. W. 1998a, *ApJS*, 117, 563  
 —. 1998b, *ApJ*, 494, L85  
 Butler, R. P., Marcy, G. W., Williams, E., McCarthy, C., Dosanjh, P., & Vogt, S. S. 1996, *PASP*, 108, 500  
 Cavallini, F., Ceppatelli, G., & Righini, A. 1985, *A&A*, 143, 116  
 Cochran, W. D., Hatzes, A. P., & Paulson, D. B. 2001, *AJ*, submitted  
 Cumming, A., Marcy, G. W., & Butler, R. P. 1999, *ApJ*, 526, 890  
 Donahue, R. A., Dobson, A. K., & Baliunas, S. L., *Solar Phys.* 171, 211  
 Dravins, D. & Nordlund, A. 1990, *A&A*, 228, 203  
 Duncan, D. K., Frazer, J., Lanning, H. H., Baliunas, S. L., Noyes, R. W., & Vaughan, A. H. 1984, *PASP*, 96, 707  
 Fekel, F. C. 1997, *PASP*, 109, 514  
 Gray, D. F. & Hatzes, A. P. 1997, *ApJ*, 490, 412  
 Hatzes, A. P., Cochran, W. D., & Bakker, E. J. 1998a, *Nature*, 391, 154  
 —. 1998b, *ApJ*, 508, 380  
 Hatzes, A. P., Cochran, W. D., & Johns-Krull, C. M. 1997, *ApJ*, 478, 374  
 Hatzes, A. P., Cochran, W. D., McArthur, B., Baliunas, S. L., Walker, G. A. H., Campbell, B., Irwin, A. W., Yang, S., Kürster, M., Endl, M., Els, S., Butler, R. P., & Marcy, G. W. 2000, *ApJ*, 544, L145  
 Henry, G. W., Baliunas, S. L., Donahue, R. A., Soon, W. H., & Saar, S. H. 1997, *ApJ*, 474, 503  
 Jeffreys, H., S. 1961, *Theory of Probability* (Oxford: Clarendon Press)  
 Kraft, R. P. 1965, *ApJ*, 142, 681  
 Kürster, M., Endl, M., Els, S., Hatzes, A. P., Cochran, W. D., Döbereiner, S., & Dennerl, K. 2000, *A&A*, 353, L33  
 Linsky, J. L. & Avrett, E. H. 1970, *PASP*, 82, 169  
 Livingston, W. 1982, *Nature*, 287, 208  
 McMillan, R. S., Moore, T. L., Perry, M. L., & Smith, P. H. 1993, *ApJ*, 403, 801  
 Middelkoop, F. 1982, *A&A*, 113, 1  
 Middelkoop, F. & Zwaan, C. 1981, *A&A*, 101, 26  
 Naef, D., Mayor, M., Pepe, F., Queloz, D., Santos, N. C., Udry, S., & Burnet, M. 2001, *A&A*, 375, 205  
 Noyes, R. W., Hartmann, L. W., Baliunas, S. L., Duncan, D. K., & Vaughan, A. H. 1984, *ApJ*, 279, 763  
 Pearson, N. S., Saar, S. H., Hatzes, A. P., & Paulsen, D. 2000, *BAAS*, Vol. 197, 1107  
 Peryman, M. A. C., Brown, A. G. A., Lebreton, Y., Gómez, A., Turon, C., Cayrel de Strobel, G., Mermilliod, J. C., Robichon, N., Kovalevsky, J., & Crifo, F. 1998, *A&A*, 331, 81  
 Queloz, D., Henry, G. W., Sivan, J. P., Baliunas, S. L., Beuzit, J. L., Donahue, R. A., Mayor, M., Naef, D., Perrier, C., & Udry, S. 2001, *A&A*, 379, 279  
 Radick, R. R., Lockwood, G. W., Skiff, B. A., & Baliunas, S. L. 1998, *ApJS*, 118, 239  
 Rutten, R. G. M. 1987, Ph.D. Thesis, 129  
 Rutten, R. G. M., Zwaan, C., Schrijver, C. J., Duncan, D. K., & Mewe, R. 1989, *A&A*, 219, 239  
 Saar, S. 2001, in *Cool Stars, Stellar Systems, and the Sun 11*, ASP Conference Series Vol. 223, ed. R. J. García López, R. Rebolo, & M. R. Zapatero Osorio, p. 292  
 Saar, S. & Osten, R. 1997, *MNRAS*, 284, 284  
 Saar, S. H. 1996, in *Stellar Surface Structure*, IAU Symp. 176, ed. J. L. K. Strassmeier (Kluwer), 237  
 Saar, S. H. 2002, in *Stellar Coronae in the Chandra and XMM-Newton Era*, ASP Conf. Series, in press, ed. F. Favata & J. Drake  
 Saar, S. H., Butler, R. P., & Marcy, G. W. 1998, *ApJ*, 498, L153, =SBM  
 Saar, S. H. & Donahue, R. A. 1997, *ApJ*, 485, 319  
 Saar, S. H. & Fischer, D. 2000, *ApJ*, 534, L105  
 Saar, S. H., Fischer, D., Snyder, N., & Smolec, R. 2001, in *Cool Stars, Stellar Systems and the Sun 11*, ASP Conf. Series, Vol. 223, CD-1051  
 Saar, S. H., Hatzes, A. P., Cochran, W. D., & Paulson, D. B. 2002, in *Cool Stars, Stellar Systems and the Sun 12*, ASP Conf. Series, in press  
 Saar, S. H. & Snyder, N. 1999, *BAAS*, Vol. 194, 10502  
 Santos, N. C., Mayor, M., Naef, D., Pepe, F., Queloz, D., Udry, S., & Blecha, A. 2000a, *A&A*, 361, 265  
 Santos, N. C., Mayor, M., Naef, D., Pepe, F., Queloz, D., Udry, S., Burnet, M., & Revaz, Y. 2000b, *A&A*, 356, 599  
 Schmitt, S. A. 1969, *Measuring Uncertainty: an Elementary Introduction to Bayesian Statistics* (Reading, Mass.: Addison-Wesley)  
 Soderblom, D. 1985, *AJ*, 90, 2103  
 Soderblom, D. R. 1982, *ApJ*, 263, 239  
 Soderblom, D. R., Duncan, D. K., & Johnson, D. R. H. 1991, *ApJ*, 375, 722  
 Strassmeier, K. G., Washuettl, A., Granzer, T., Scheck, M., & Weber, M. 2000, *A&AS*, 142, 275  
 Tinbergen, J. & Zwaan, C. 1981, *A&A*, 101, 223  
 Valenti, J. A., Butler, R. P., & Marcy, G. W. 1995, *PASP*, 107, 966  
 Vogt, S. S., Allen, S. L., Bigelow, B. C., Bresee, L., Brown, B., Cantrall, T., Conrad, A., Couture, M., Delaney, C., Epps, H. W., Hilyard, D., Hilyard, D. F., Horn, E., Jern, N., Kanto, D., Keane, M. J., Kibrick, R. I., Lewis, J. W., Osborne, J., Pardeilhan, G. H., Pfister, T., Ricketts, T., Robinson, L. B., Stover, R. J., Tucker, D., Ward, J., & Wei, M. Z. 1994, *Proc. Soc. Photo-opt. Inst. Eng.*, 2198, 362

Vogt, S. S., Butler, R. P., Marcy, G. W., Fischer, D. A., Pourbaix, D., Apps, K., & Laughlin, G. 2002, *ApJ*, 568, 352  
 Walker, G. A. H., Bohlender, D. A., Walker, A. R., Irwin, A. W., Yang, S. L. S., & Larson, A. 1992, *ApJ*, 396, L91

Walker, G. A. H., Walker, A. R., Irwin, A. W., Larson, A. M., Yang, S. L. S., & Richardson, D. C. 1995, *Icarus*, 116, 359

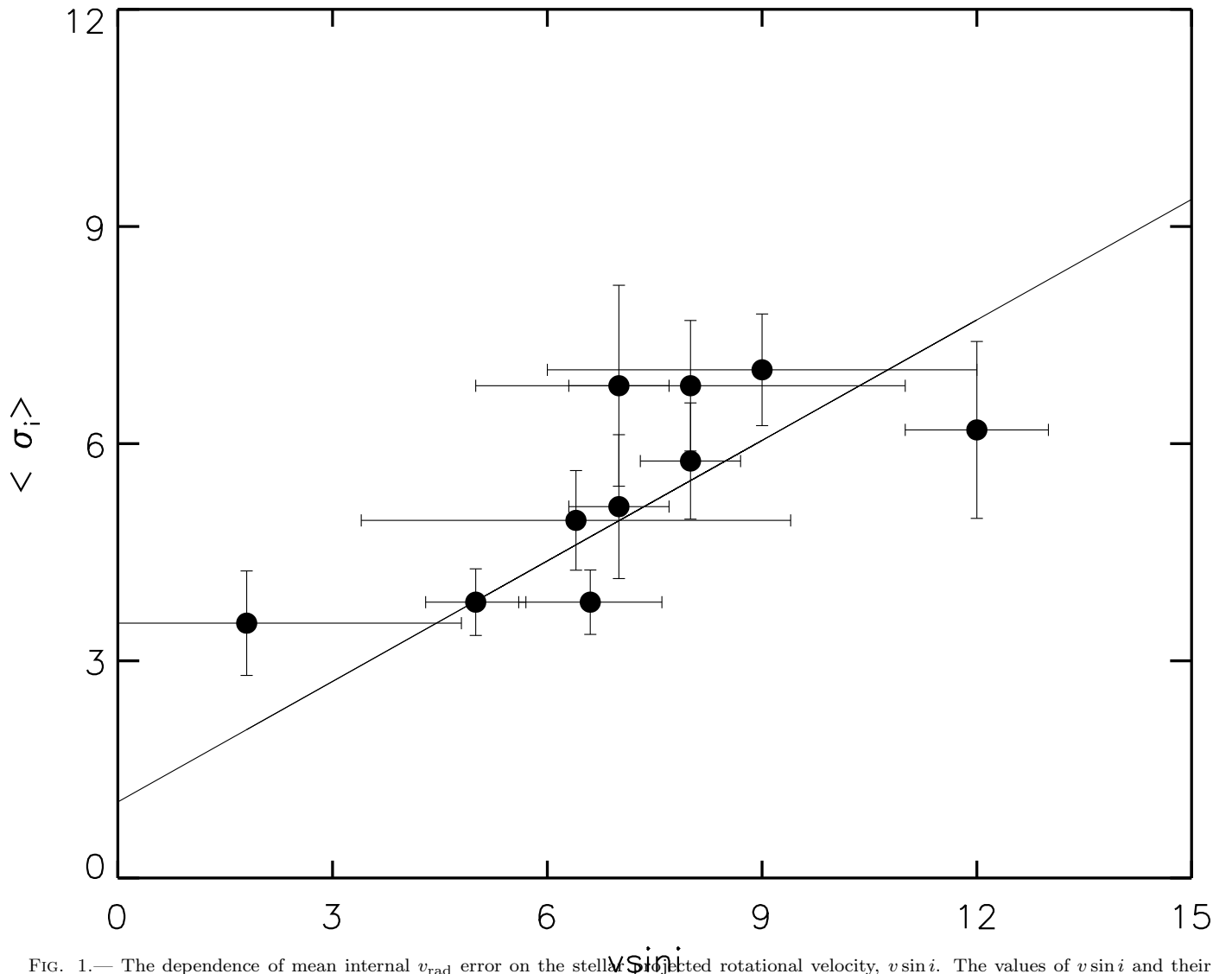


FIG. 1.— The dependence of mean internal  $v_{\text{rad}}$  error on the stellar projected rotational velocity,  $v \sin i$ . The values of  $v \sin i$  and their sources are listed in Table 1. Vertical error bars indicate the standard deviation from the mean for all of our velocity measurements for a given star.

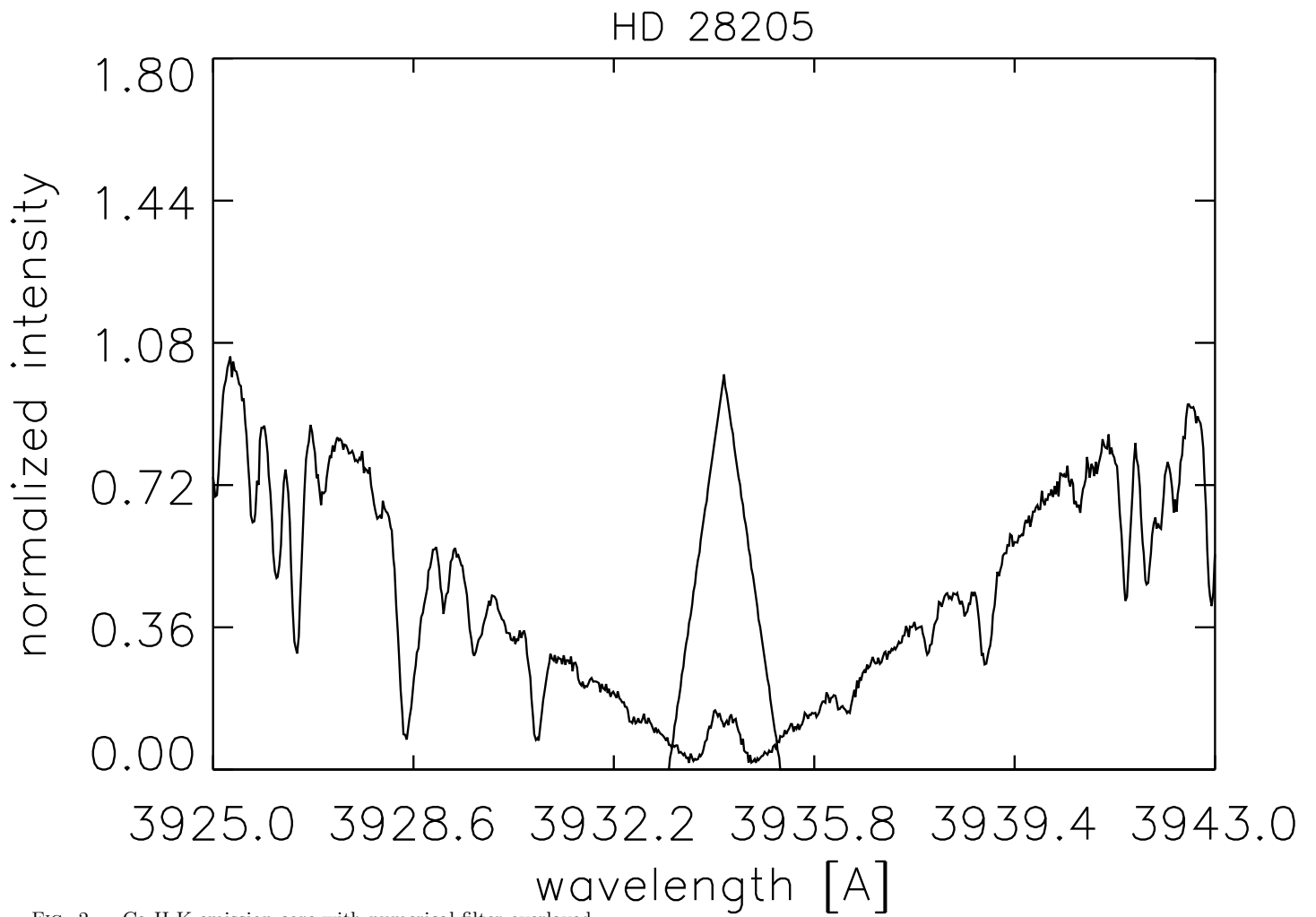


FIG. 2.— Ca II K emission core with numerical filter overlaid



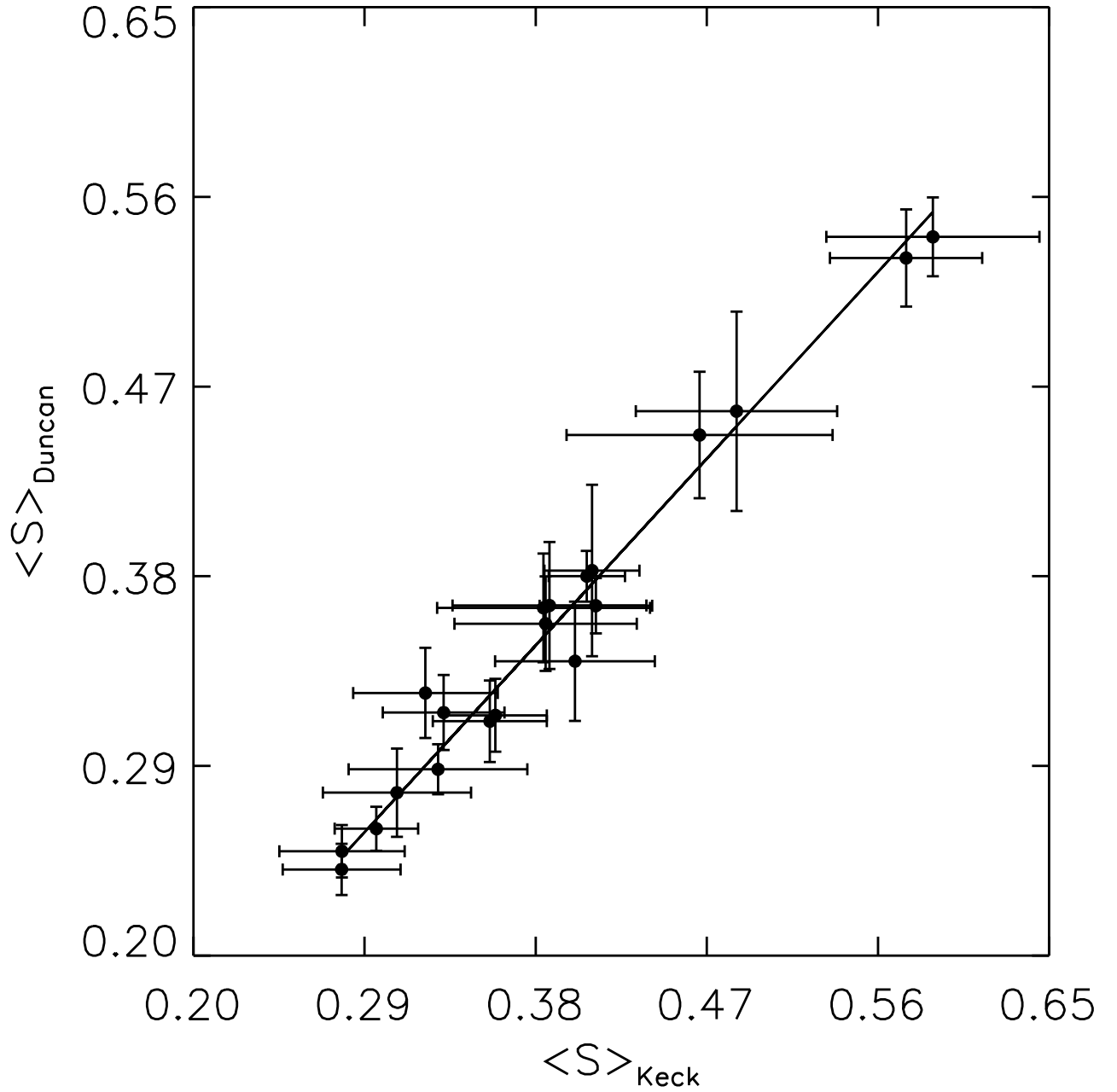


FIG. 3.— Comparison of our computed S index with published values from Duncan et al. (1984). The straight line is the linear fit discussed in section 2.3. Error bars indicate the rms about the mean S value for each star.

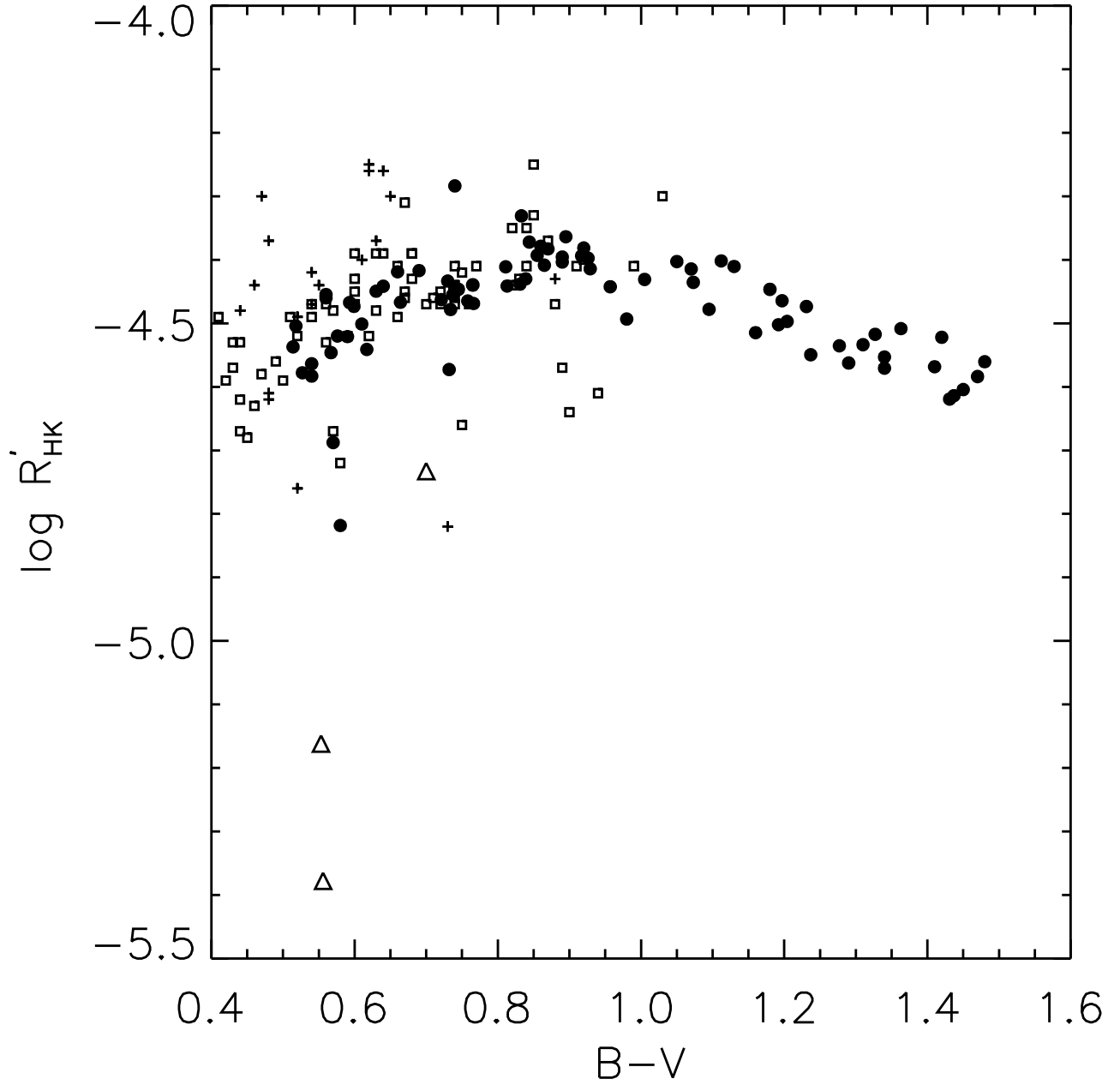


FIG. 4.—  $R'_{HK}$  vs.  $B-V$ . Filled circles=Our Hyades program stars. Open triangles= Members according to Perryman et al. (1998) but are non-members due to high Hipparcos distances, photometry below the main-sequence and velocities which disagree with members according to D. Latham (private communication). Open squares=Rutten (1987) Hyades data. Crosses=Rutten (1987) Pleiades data.

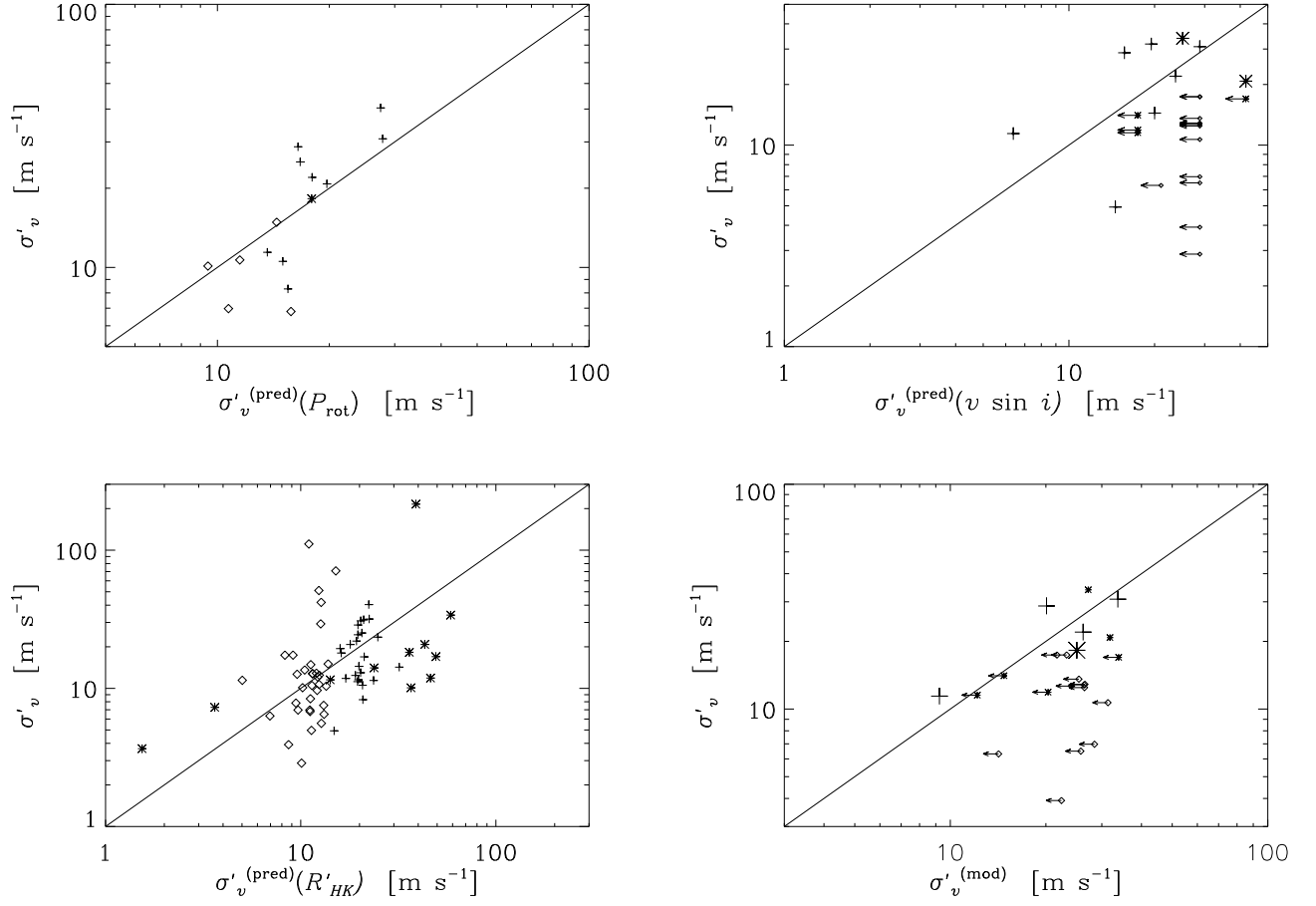


FIG. 5.— Comparison between measured  $\sigma'_v$  for our stars, and predicted  $\sigma'_v$  based on empirical based on relations (see SBM) between  $\sigma'_v$  and  $P_{\text{rot}}$  (top left),  $v \sin i$  (top right) and  $R'_{\text{HK}}$  (bottom left; separate fits for G and K stars used). Bottom right shows comparison between  $\sigma'_v$  (Hyades) and those predicted by the simple spot/plage model in SBM (smaller symbols have estimated  $P_{\text{rot}}$ ). In each case, F, G, and K stars are given by \*, +, and diamonds, respectively, and the solid line indicates the observed  $\sigma'_v = \sigma'_v$  (pred.).

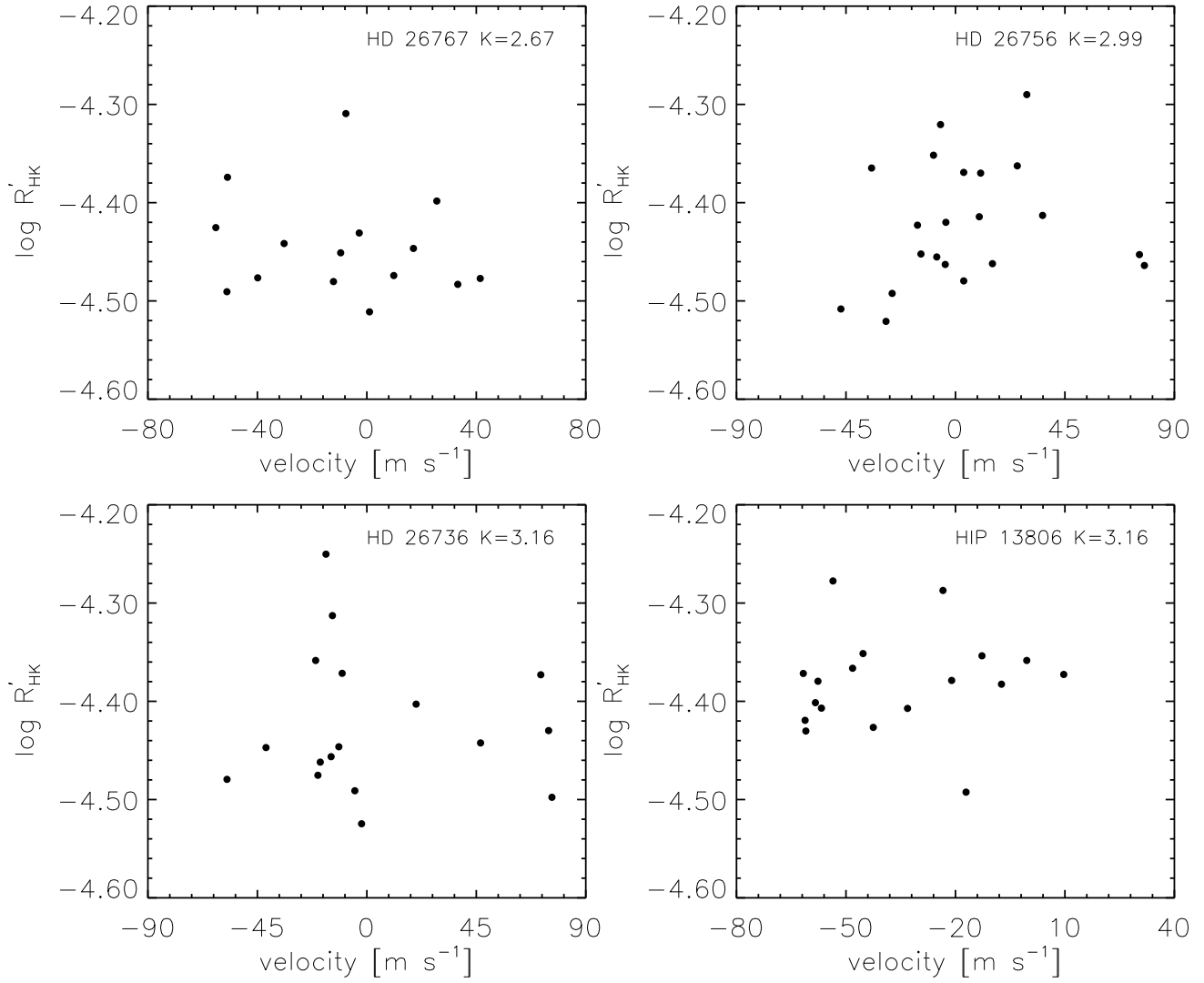


FIG. 6.— Examples of stars showing uncorrelated trends in  $\log R'_{HK}$  vs. radial velocity.

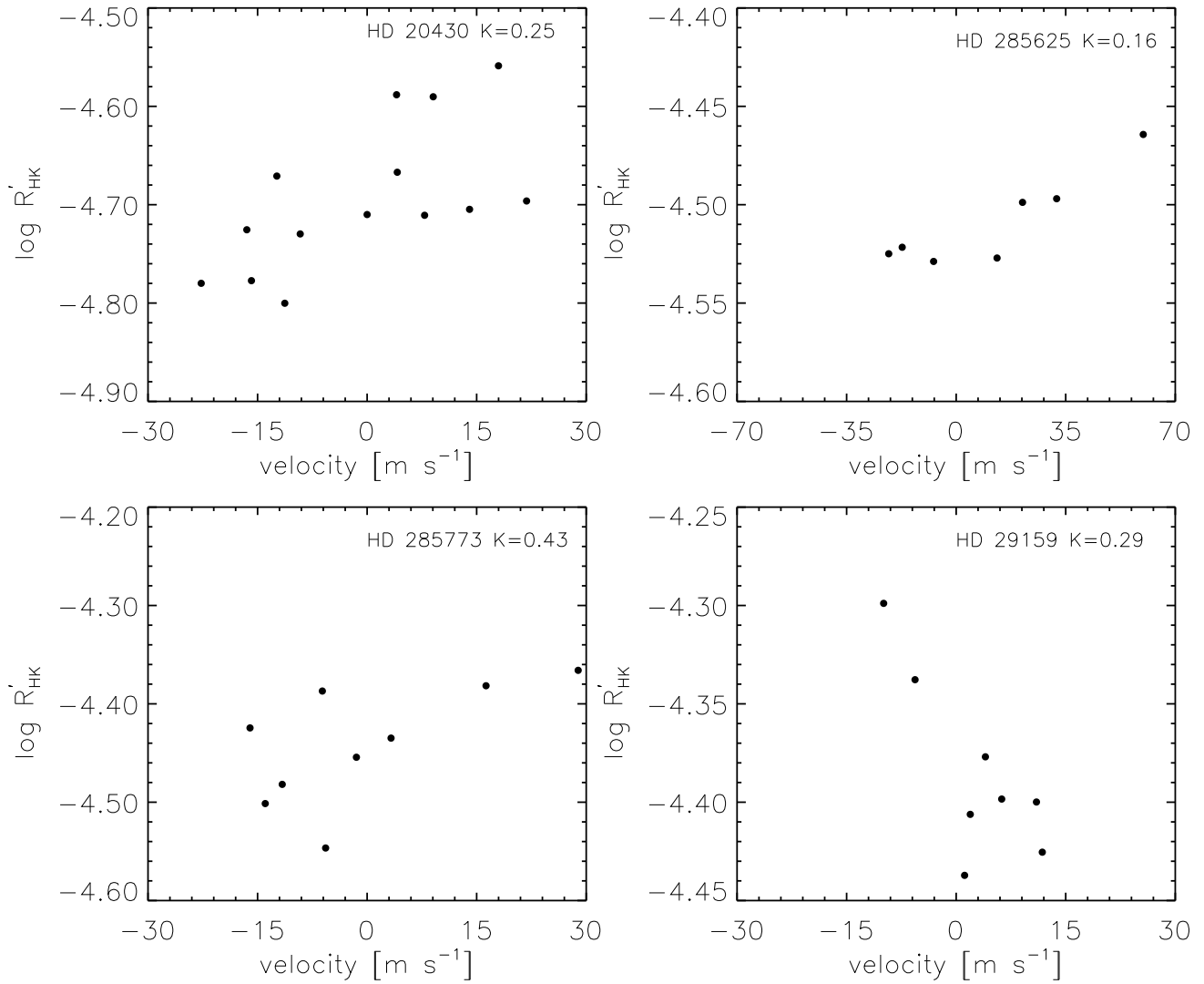


FIG. 7.— Examples of stars showing correlated trends in  $\log R'_{HK}$  vs. radial velocity.

TABLE 1  
INTERNAL ERRORS VERSUS ROTATION FOR THE PROGRAM STARS

HD	Other Name	$v \sin i$ [km s <sup>-1</sup> ]	$\langle \sigma_i \rangle$ [m s <sup>-1</sup> ]	Reference ]
18632	BD+07 459	1.8±1.0	3.52±0.72	1
26756	vB 17	6.4±3.0	4.94±0.69	2
26736	vB 15	7.0±0.7	5.13±0.99	3
27282	vB 27	6.6±3.0	3.81±0.45	2
27406	vB 31	12.0±1.0	6.19±1.22	3
27859	vB 52	8.0± 0.7	5.76±0.80	3
20899	vB 64	5.0±0.7	3.81±0.46	3
28205	vB 65	9.0±3.0	7.02±0.77	4
28237	vB 66	8.0±3.0	6.80±0.90	4
28344	vB 73	7.0±0.7	6.80±1.39	3

References. — (1) Fekel (1997); We adopted an error of 1.0 km s<sup>-1</sup>. (2) Strassmeier et al. (2000); We adopted errors of 3.0 km s<sup>-1</sup>. (3) Soderblom (1982) (4) Kraft (1965); We adopted errors of 3.0 km s<sup>-1</sup>.

TABLE 2  
COMPARISON OF OBSERVED AND PREDICTED/MODELED  $\sigma'_v$

Type of Fit/Model <sup>1</sup>	Spec. type studied	$N$	$\langle \sigma'_v(\text{pred.}) - \sigma'_v \rangle$ [dex]	$\sigma_{rms}$ [dex]	$\sigma_{rms}(\text{Lick})^2$ [dex]
$R'_{\text{HK}}(\text{F})$	F	11	0.124	0.444	0.41
$R'_{\text{HK}}(\text{F})$	F <sup>3</sup>	10	0.210	0.376	0.41
$R'_{\text{HK}}(\text{G})$	F <sup>3</sup>	10	-0.107	0.213	...
$R'_{\text{HK}}(\text{G+K})$	F <sup>3</sup>	10	-0.213	0.284	...
$R'_{\text{HK}}(\text{G+K})$	G	24	-0.045	0.216	...
$R'_{\text{HK}}(\text{G+K})$	K	34	0.117	0.348	...
$R'_{\text{HK}}(\text{G+K})$	K <sup>3</sup>	33	0.146	0.320	...
$R'_{\text{HK}}(\text{G+K})$	G+K	58	0.050	0.298	0.25
$R'_{\text{HK}}(\text{G+K})$	G+K <sup>3</sup>	57	0.065	0.278	0.25
$R'_{\text{HK}}(\text{G})$	G	24	0.073	0.224	...
$R'_{\text{HK}}(\text{K})$	K	34	-0.040	0.329	...
$R'_{\text{HK}}(\text{K})$	K <sup>3</sup>	33	-0.011	0.284	...
$v \sin i(\text{F})$	F	3	0.125	0.263	0.31
$v \sin i(\text{G+K})$	G <sup>4</sup>	7	-0.016	0.265	0.22
$P_{\text{rot}}(\text{F})$	F	1	-0.008	...	0.35
$P_{\text{rot}}(\text{G+K})$	G+K	14	0.021	0.176	0.22
model	F+G <sup>4</sup>	5	0.001	0.121	0.14
model <sup>5</sup>	F+G <sup>4</sup>	7	0.013	0.130	0.16

<sup>1</sup>e.g.,  $R'_{\text{HK}}(\text{G+K})$  indicates that the  $\sigma'(\text{pred.})$  based on the empirical fit for G and K stars of  $\sigma'_v(\text{Lick})$  vs.  $R'_{\text{HK}}$  (from SBM) is compared to Hyades stars of the spectral type listed in column (2). Note: separate G star ( $\propto R'_{\text{HK}}{}^{1,15}$ ) and K star ( $\propto R'_{\text{HK}}{}^{1,19}$ ) fits for  $R'_{\text{HK}}$  based on Lick data were not listed in SBM.

<sup>2</sup>from SBM

<sup>3</sup>with one outlier removed

<sup>4</sup>No Hyad K dwarfs in our sample have published  $v \sin i$  measurements

<sup>5</sup>Assuming  $f_S = 0$  for F stars

TABLE 3  
PROGRAM INFORMATION

HD or HIP #	Other Name	# obs.	B-V	$\langle R'_{HK} \rangle$	$\sigma_{<R'_{HK}>}$	$r$	$P_c(R'_{HK}, r)$	$K(r^2)$
HD 14127	BD+04 378	12	0.567	2.84	0.38	0.55	0.07	0.66
HIP 13600	BD+17 455	10	0.704	1.85	0.31	-0.08	0.83	2.41
HIP 13806	vB 153	18	0.855	4.18	0.49	0.09	0.73	3.16
HD 18632	BD+07 459	9	0.926	4.00	0.52	0.00	1.00	2.33
HD 19902	BD+32 582	10	0.732	2.67	0.40	0.07	0.85	2.43
HD 20430	vB 1	13	0.567	2.07	0.37	0.62	0.02	0.25
HD 20439	vB 2	13	0.617	2.88	0.31	0.30	0.33	1.79
HIP 15563	BD+07 499	9	1.130	3.89	0.38	-0.60	0.09	0.62
HIP 15720	...	8	1.431	2.40	0.18	0.10	0.82	2.14
HIP 16529	vB 4	9	0.844	4.25	0.36	0.13	0.73	2.21
HIP 16908	vB 5	10	0.917	4.04	0.38	0.32	0.36	1.77
HD 23453	BD+25 613	8	1.437	2.43	0.22	-0.27	0.51	1.87
HIP 17766	G7-15	7	1.340	2.69	0.29	0.02	0.96	2.03
HIP 18018	vB 170	11	1.160	3.06	0.36	0.30	0.38	1.79
HD 286363	BD+12 524	7	1.070	3.85	0.45	0.06	0.90	2.02
HD 25825	vB 7	8	0.895	4.33	0.36	0.19	0.65	2.03
HIP 18946	BD+19 650	7	1.095	3.33	0.47	0.23	0.62	1.82
HIP 19082	L 12	7	1.347	2.80	0.29	0.61	0.15	0.81
HD 285367	BD+17 679	8	0.890	4.02	0.24	0.29	0.48	1.82
HD 25825	vB 10	8	0.593	3.41	0.47	0.20	0.63	2.01
HD 285507	J 231	8	1.180	3.58	0.35	0.41	0.31	1.50
HIP 19261B	vB 12	8	0.740	5.20	0.59	-0.01	0.98	2.18
HD 285482	BD+16 558	7	1.005	3.71	0.29	-0.30	0.52	1.69
HD 286554	J 233	7	1.327	3.04	0.24	0.11	0.82	1.99
HD 26257	BD-00 648	9	0.553	0.69	0.20	-0.51	0.16	0.95
HIP 19441	BD+08 642	6	1.192	3.15	0.29	0.33	0.52	1.67
HD 26756	vB 17	21	0.693	3.83	0.57	0.14	0.53	2.99
HD 26767	vB 18	15	0.640	3.62	0.47	-0.15	0.60	2.67
HD 26736	vB 15	17	0.657	3.81	0.68	-0.06	0.82	3.16
HD 26784	vB 19	11	0.514	2.90	0.42	-0.12	0.73	2.45
HD 286589	vA 68	7	1.204	3.18	0.44	0.09	0.85	2.00
HD 285625	vA 72	8	1.363	3.06	0.21	0.86	0.01	0.16
HD 285590	vA 75	7	1.290	2.74	0.16	0.17	0.71	1.92
...	vA 115	6	1.470	2.61	0.31	0.73	0.10	0.87
HD 285690	vB 25	7	0.980	3.21	0.23	0.39	0.39	1.48
...	vA 146	6	1.420	3.01	0.34	0.56	0.24	1.27
HD 27250	vB 26	8	0.745	3.58	0.35	-0.07	0.87	2.16
HD 27282	vB 27	9	0.721	3.45	0.64	0.53	0.14	0.86
HD 27406	vB 31	8	0.560	3.51	0.79	0.31	0.46	1.79
HD 27732	vB 42	8	0.758	3.43	0.23	0.33	0.42	1.73
HIP 20485	vB 173	6	1.231	3.36	0.20	-0.07	0.89	1.86
HD 27771	vB 46	8	0.855	4.05	0.33	-0.24	0.56	1.94
HD 27835	vB 49	8	0.590	3.01	0.62	-0.20	0.63	2.01
HD 27808	vB 48	8	0.518	3.13	0.38	0.28	0.50	1.85
HIP 20485	vB 174	7	1.050	3.96	0.50	0.08	0.86	2.01
HD 27859	vB 52	9	0.599	3.36	0.50	0.14	0.73	2.20
...	vA 354	7	1.310	2.93	0.40	0.41	0.35	1.39
...	vA 383	6	1.450	2.49	0.20	0.03	0.95	1.87
HD 20899	vB 64	9	0.664	3.41	0.39	0.14	0.72	2.19
HD 28205	vB 65	8	0.537	2.61	0.44	0.10	0.82	2.15
HD 28237	vB 66	8	0.560	3.47	0.63	0.26	0.53	1.89
HD 285830	vB 179	8	0.929	3.85	0.32	0.35	0.40	1.69
HD 28258	vB 178	9	0.839	3.72	0.36	-0.48	0.19	1.07
HD 28344	vB 73	10	0.609	3.15	0.60	0.21	0.56	2.15
...	vA 502	6	1.410	2.70	0.15	-0.47	0.35	1.47
HD 283704	vB 76	10	0.766	3.40	0.40	-0.12	0.73	2.35
HD 285773	vB 79	9	0.831	3.64	0.49	0.66	0.06	0.43
HD 28462	vB 180	7	0.865	3.90	0.63	-0.39	0.39	1.46
HD 28593	vB 87	9	0.734	3.32	0.68	0.11	0.77	2.24
HD 28635	vB 88	10	0.540	2.73	0.57	0.69	0.03	0.34
...	vA 637	6	1.480	2.75	0.18	-0.52	0.29	1.36
HD 28805	vB 92	7	0.740	3.59	0.29	0.09	0.84	2.00
HD 284552	L 66	6	1.237	2.82	0.41	0.55	0.26	1.31
HD 28878	vB 93	8	0.890	3.95	0.56	-0.39	0.34	1.56
HD 285837	L 65	6	1.197	3.43	0.51	0.77	0.07	0.77
HD 28977	vB 183	7	0.920	4.16	0.61	0.06	0.90	2.02
HD 28892	vB 97	8	0.631	3.55	0.49	-0.29	0.49	1.84
HD 29159	vB 99	8	0.870	4.14	0.46	-0.80	0.02	0.29
HD 29419	vB 105	8	0.576	3.02	0.78	-0.24	0.56	1.93
HD 286929	J 311	6	1.073	3.67	0.35	0.71	0.12	0.93
HD 284574	vB 109	7	0.811	3.88	0.71	-0.21	0.65	1.86
HIP 22177	J 326	6	1.277	2.91	0.09	0.70	0.12	0.95
HD 284653	J 330	6	1.112	3.96	0.23	-0.45	0.38	1.50
HD 30505	vB 116	9	0.833	4.67	0.88	-0.39	0.30	1.42
HD 30589	vB 118	10	0.578	1.52	0.28	-0.24	0.50	2.04
HD 30809	vB 143	7	0.527	2.64	0.50	-0.29	0.54	1.72
HD 31609	vB 127	7	0.737	3.51	0.50	-0.10	0.84	1.99
...	BD+04 810	6	0.957	3.61	0.23	-0.43	0.39	1.52
HD 32347	vB 187	7	0.765	3.64	0.57	-0.12	0.80	1.98
HD 240648	BD+17 841	7	0.730	3.69	0.24	0.25	0.59	1.79
HD 242780	BD+11 772	6	0.765	3.63	0.23	0.81	0.05	0.63
HD 35768	BD+32 955	6	0.556	0.42	0.17	0.16	0.76	1.82